Analysis of Tunnel Face Stability of Shield Tunneling Through Water-Rich Sand-Pebble Stratum

Wei Wang, Fan Liu(✉), Zhao Han, Xinyuan Zhang, and Xu Zhou

School of Civil Engineering, Central South University, Changsha 410075, China

Abstract. The sand and pebble stratum generally exists in the urban underground engineering construction. When disturbed by the outside world, especially under the condition of rich water, it is easy to cause stratum loss due to the characteristics of sand pebble stratum, resulting in instability of the face and surface settlement and other problems. In this paper, the physical and mechanical parameters of sand pebble soil in a subway area of Changsha were obtained through laboratory tests, and then the micro parameters were calibrated. According to the calibrated micro parameters, a PFC^{3D} full scale model considering seepage was established for the stability analysis of the tunnel face. Through the analysis of the numerical simulation results, the influence of different factors such as stress ratio, buried depth (C), shield diameter (D), and boulders on the stability of the tunnel face was obtained, and the variation characteristics of the limit support pressure and the critical stress ratio of the instability index were obtained under different conditions. The results show that the formation stability increases with the increase of stress ratio in the process of shield tunneling. When the stress ratio is less than the critical stress ratio, the tunnel face will be unstable. When the boulder is broken, the instantaneous velocity of the particle in the center of the tunnel surface can reach 3m/s, and the risk of instability of the tunnel surface is increased. The pressure of the limit support increases with the increase of the buried depth. When C/D = 3, the pressure of the limit support tends to be stable. The critical stress ratio decreases with the increase of C/D, and the lower the critical stress ratio is, the stronger the self-stabilizing ability of the tunnel surface is.

Keywords: Shield tunnel · Sandy pebble stratum · Micro analysis · Face stability

1 Introduction

As the main construction method of underground traffic structure, shield is widely used in urban rail transit engineering. In recent years, during the construction of underground projects in many cities, sand and pebble stratum have often been encountered. Due to the large gaps between the particles, small cohesion, large permeability coefficient and high sensitivity, when subjected to external disturbances, it is easy to form a point-to-point force transmission state between the particles. Therefore, for tunnel construction under this stratum, the stability of the face is difficult to control, and related engineering accidents are common.

Y. Liu et al. (Eds.): GeoChina 2021, SUCI, pp. 112–131, 2021.
https://doi.org/10.1007/978-3-030-80316-2_11

Regarding the tunnel face stability of shield tunneling through sand-pebble stratum, scholars have carried out researches on theoretical analysis, laboratory tests and numerical simulations. In terms of numerical simulation, finite element and discrete element are mainly two analysis methods. In terms of finite element analysis, Vermeer et al. [1] studied the relationship between the ultimate supporting force at the tunnel face and the soil parameters (internal friction angle, etc.) under drainage conditions; Zhang et al. [2] proposed a new shield tunnel instability Mechanism, and analyzed the influence of tunnel depth and soil properties on the stability of the tunnel face. In terms of discrete element analysis, Melis et al. [3–6] with the help of PFC^{3D}, studied the change law of the excavation parameters of the earth pressure shield and the stability of the tunnel face, and further studied the stability of the tunnel face during the sand excavation process of the earth pressure shield tunnel; KIRSCHA et al. [7–9] studied the related factors of tunnel face instability and their influence sensitivity; Some scholars used discrete element software to establish the sand-pebble mesoscale model, studied the stability of the tunnel face in the process of shield tunneling, and compared the calculation results with theoretical analytical values [10–13]. However, in terms of the instability of palm surface, the seepage action of water is not considered in most relevant studies, and the sand pebble formation soil particles are greatly simplified, which makes the sand pebble formation mesoscale model may be greatly different from the actual situation.

Based on the Changsha Metro Line 3, according to the parameters of sandy pebble soil obtained in laboratory tests, aiming at the deformation characteristics of sandy pebble soil in mesoscale during shield tunneling, this paper establish a multi-phase mesoscale simulation model of sandy pebble soil considering gradation characteristics and permeability to analyze the change characteristics of sandy pebble soil in front of palm during shield tunneling. This study did not aim to supply quantitative application for specific construction sites, but paid more attention to a general investigation of the behavior about tunnel face stability of shield tunneling through water-rich sand-pebble stratum.

2 Laboratory Test Analysis

2.1 Particle State Analysis of Sandy Pebble Soil

Five sandy pebble samples were selected from different locations within the scope of the project, and the statistical samples are shown in Fig. 1. Each sample contains 30 randomly selected particles. Measure the long diameter (a), medium diameter (b) and short diameter(c) of each sandy pebble. According to the measurement results, calculate the flatness (F) and sphericity (Ψ) of each group of sand and gravel particles in turn. The data results are as follows Table 1.

$$F = \frac{a + b}{2c} \tag{1}$$

$$\psi = \frac{\sqrt[3]{abc}}{a} \tag{2}$$

Fig. 1. Statistical pattern of sand pebble size

Table 1. Particle state characteristics of each sample

Particle state	Sample number				
	1#	2#	3#	4#	5#
F	1.54	1.57	1.44	1.55	1.53
Ψ	0.76	0.75	0.79	0.75	0.76
F/Ψ	2.03	2.09	1.82	2.07	2.01

It can be seen from Table 1 that the flatness and sphericity are between 1.44–1.57 and 0.75–0.79 respectively, and the ratio of them is basically stable at about 2, indicating that the morphological differences of each sample are very small and most of them are oblate bodies.

2.2 Sandy Pebble Soil Screening Experiment

The grading curve of sandy pebble soil samples taken in this research is shown in Fig. 2. It can be seen from Fig. 2 that the particle size can be roughly divided into three groups: 0–20 mm, 20–40 mm, and 40–80 mm, each accounting for about 1/3.

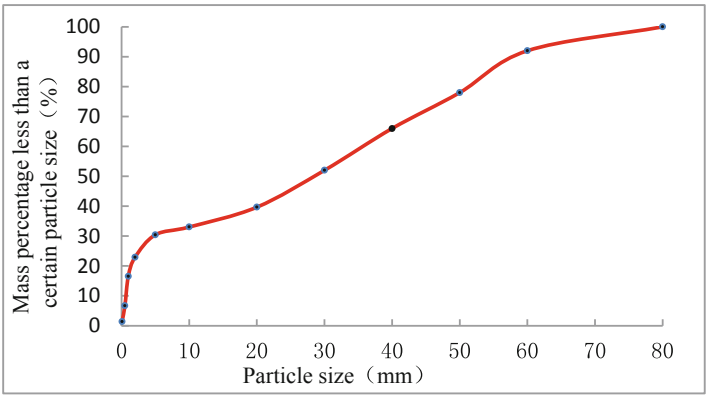

Fig. 2. Grading curve of sandy pebble soil sample

2.3 Sandy Pebble Soil Permeability Test

In this paper, 15 groups of sandy pebble soil with different gradations are carried out and analyzed to study the relationship between effective size (d_{10}), uniformity coefficient (C_u), curvature coefficient (C_c) and permeability coefficient, and then obtain the empirical formula of permeability coefficient and the three.

(1) Effect of d_{10} on permeability coefficient (K_1)

If Cu and Cc are constant, d10 becomes the only variable that affects the permeability coefficient. So in this part we take Cu = 28.5 and Cc = 0.64, the specific working condition design is shown in Table 2 below.

Table 2. Interval content of each particle size group under different d_{10}

Particle size (mm)	$C_u = 28.5$ $C_c = 0.64$				
	$d_{10} = 0.175$ mm	$d_{10} = 0.275$ mm	$d_{10} = 0.375$ mm	$d_{10} = 0.5625$ mm	$d_{10} = 0.75$ mm
0.1–0.25	10	5	5	3	2
0.25–0.5	20	15	10	5	5
0.5–1.0	30	25	20	15	10
1.0–2.0	40	40	29	20	20
2.0–5.0	50	50	40	31	29
5.0–10.0	70	60	45	40	35
10.0–20.0	80	80	80	45	40
>20.0	100	100	100	100	100

Determine the permeability coefficient (the slope of the fitting straight line) according to the V-J (velocity-hydraulic gradient curve) of the sample under each working condition. The results are shown in Table 3.

Table 3. Permeability coefficient under different d_{10}

Constant	$C_u = 28.5$ $C_c = 0.64$				
Effective particle size (mm)	0.175	0.275	0.375	0.5625	0.75
Permeability coefficient *K* (cm/s)	0.0056	0.0248	0.0591	0.2653	0.8288

Then, we use different functions fit the permeability coefficient and d10, and we find that when the power function is used to fit the two variables, the correlation between the two variables is the highest, reaching 0.9963. Therefore, the fitting equation of K1 and d10 is:

$$K_1 = 1.957 d_{10}^{3.4044}$$

(2) Effect of C_u on permeability coefficient (K_2)

Using the same method as above, taking d10 = 0.375 and Cc = 0.83, the fitting equation of K2 and Cu is obtained as:

$$K_2 = -0.008 \ln C_u + 0.0641$$

(3) Effect of C_c on permeability coefficient (K_3)

Using the same method as above, taking $d_{10} = 0.375$ and $C_u = 20$, the fitting equation of K_3 and C_c is obtained as:

$$K_3 = 0.0023 C_C^2 - 0.007 C_c + 0.0336$$

(4) Formula establishment of Sandy pebble soil permeability coefficient (K)

From the above research, we can see that K has a nonlinear relationship with d_{10}, C_u, C_c. Based on the above conclusions, an empirical formula model is established as:

$$K = aK_1K_2K_3 + bK_1K_2 + cK_1K_3 + dK_2K_3 + eK_1 + fK_2 + gK_3 + h$$

Where a–h = model parameters.

Substituting 15 sets of data into the above formula, a linear equation system with K and 8 parameters is obtained. The equation system contains 15 linear equations. Solving the equation system through Matlab, the result is as shown.

$$K = -6.39 \times 10^4 K_1K_2K_3 - 411K_1K_2 + 377K_1K_3 - 74K_2K_3 + 77K_1 + 162K_2 + 154K_3 - 11$$

2.4 Sandy Pebble Triaxial Compressive Test

Through the triaxial compressive test (No drainage, axial load, strain control, strain rate is about 0.5%/min, confining pressure is selected as 100/200/400 MPa), the relationship between deviatoric stress and axial strain under different confining pressures is obtained, as shown in Fig. 3. And further draw the mohr's stress circle, as shown in Fig. 4.

According to the indoor triaxial compressive test, the macro-physical and mechanical parameters shown in Table 4 are obtained, which provides a reference for the calibration of numerical simulation parameters in the subsequent chapters.

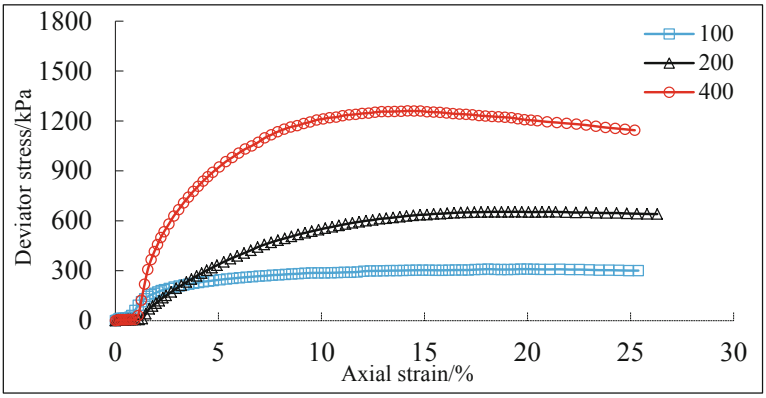

Fig. 3. Sandy pebble soil stress-strain curve under different confining pressure

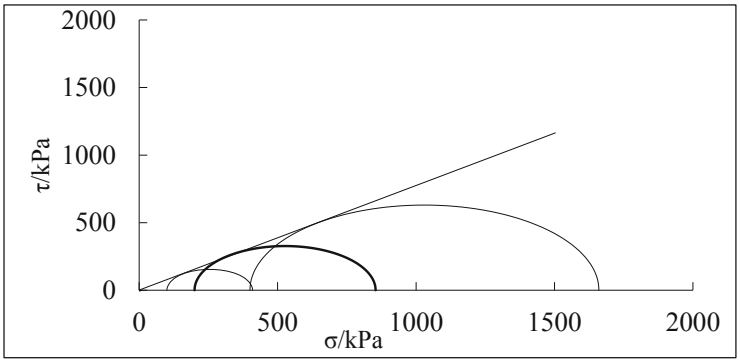

Fig. 4. Sandy pebble soil mohr's stress circle

Table 4. Macroscopic physical and mechanical parameters of Sandy pebble soil

Material name	Density (Kg/m^3)	Elastic Modulus (MPa)	Poisson's ratio	Internal friction angle	Cohesion (KPa)
Sandy pebble soil	2150	45	0.2	37.7	1.4

3 Numerical Modeling

3.1 Model Parameter Calibration

Use the PFC^{3D} software FISH language programming to build the model. The three-axis model should maintain the same meso-parameters as the subsequent engineering full-scale model, otherwise the parameter calibration through the triaxial compressive test will be meaningless. However, if the model is modeled according to the actual

gradation and actual particle size, the amount of particles generated by the subsequent shield tunneling model will reach 100 million, and the software cannot calculate it. It can only match the computer's calculation efficiency by controlling the number of particles. Therefore, it is necessary to simplify and enlarge the gradation and particle size of the particles, but in order to better reflect the stratum gradation relationship, this article will roughly divide the particles into three particle size ranges according to the gradation curve in Fig. 2. And enlarge the particle size roughly ten times, as shown in Table 5.

Table 5. Correspondence between model and actual particle size

Actual particle size range	<20 mm	20–40 mm	>40 mm
Model particle size range	100–200 mm	200–400 mm	400–600 mm

Through the analysis of macro and micro parameters of sandy pebble soil, the simulation parameters suitable for the micro model were selected, and the corresponding numerical triaxial test was carried out by comparing with the indoor triaxial test (the comparison of results is shown in Fig. 5) to determine the simulation parameters. In addition, the permeability related parameters were determined by the analysis of permeability test. The parameters of each micromodel are shown in Table 6.

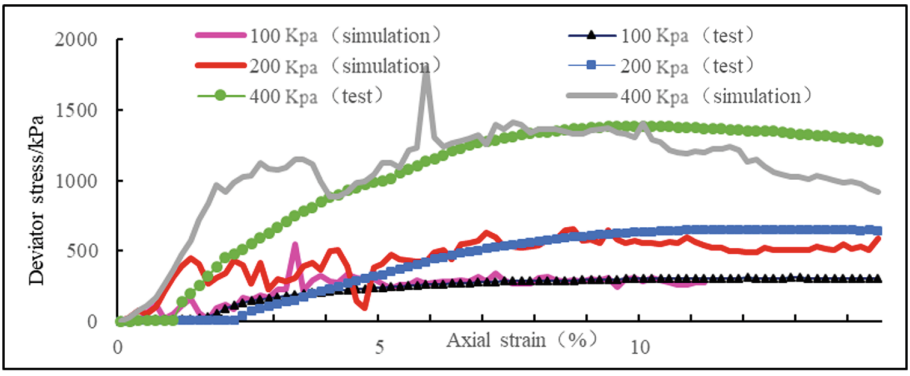

Fig. 5. Deviatoric stress-axial strain relationship diagram

Table 6. Sandy pebble soil Microscopic physical and mechanical parameters

Parameter name	P Kg/m^3	R/m	μ	K_n/(N/m)	K_t/(N/m)	bs/Mpa	r	Pw Kg/m^3	K m/s
Value	3300	0.05–0.3	10	200	3	0.2	0.15	1000	0.016

3.2 Analysis Model Establishment

According to the range of 35 m (transverse) × 20 m (longitudinal) × 40 m (high) in the actual formation, and the water level is 3 m below the surface. Use the built-in CFD of PFC and Python script to set the flow field of the corresponding water level, the flow pressure gradient is 0.02 m, the analysis model as shown in Fig. 6 is established.

Combining the actual engineering and simulation conditions, through the control variable method, a total of 13 full-scale simulation conditions are set for different factors, as shown in Table 7.

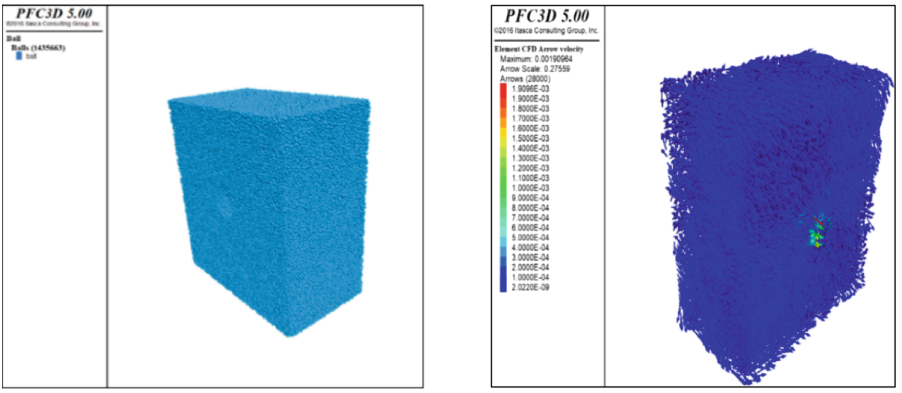

(a) Model particle generation diagram (b) Seepage flow field setting diagram

Fig. 6. Analysis model

Table 7. Full-scale simulation conditions

Serial number	Influencing factors					
	Stress ratio	D (m)	C (m)	C/D	Boulder	Remarks
1	0.5	6	15	2.5	None	Basic conditions
2	0.1	6	15	2.5	None	Influence of stress ratio (λ)
3	0.2	6	15	2.5	None	
4	0.3	6	15	2.5	None	
5	0.4	6	15	2.5	None	
6	0.6	6	15	2.5	None	
7	0.7	6	15	2.5	None	
8	0.8	6	15	2.5	None	
9	0.5	9	15	1.7	None	Influence of shield diameter
10	0.5	15	15	1	None	
11	0.5	6	6	1	None	Influence of buried depth
12	0.5	6	30	5	None	
13	0.5	6	15	2.5	Exist	Influence of Boulder

4 Discussion and Analysis

The stability of the tunnel face is actually attributed to the relationship between the shield cutter head support pressure and the limit value of the tunnel face instability. In other words, when the support pressure is greater than the limit support pressure, the stability of the tunnel face can be guaranteed. Therefore, the subsequent analysis can study the influence of various factors on the limit support pressure according to this idea. Two concepts are introduced here: (1) Stress ratio (λ): The ratio of the cutter head support pressure to the original horizontal stress of the formation at the center of the cutter head (including water pressure when containing water). Compared with simply analyzing the size of the supporting force, the value of the stress ratio is between 0 and 1, the change range is small, it is easier to grasp its regularity, and it is more valuable for engineering application and promotion. (2) Critical stress ratio: the minimum value of stress ratio that does not cause tunnel face instability (significant increase in particle displacement and velocity). The value of the critical stress ratio multiplied by the original horizontal stress of the tunnel face represents the ultimate support pressure required to ensure the stability of the tunnel face under this working condition. The influence of various factors on the critical stress ratio can also be very good. Reflecting the influence of various factors on the stability of the face, it is more feasible to study the critical stress ratio to reflect the stability of the face.

4.1 Influence of λ on Stability of Tunnel Face

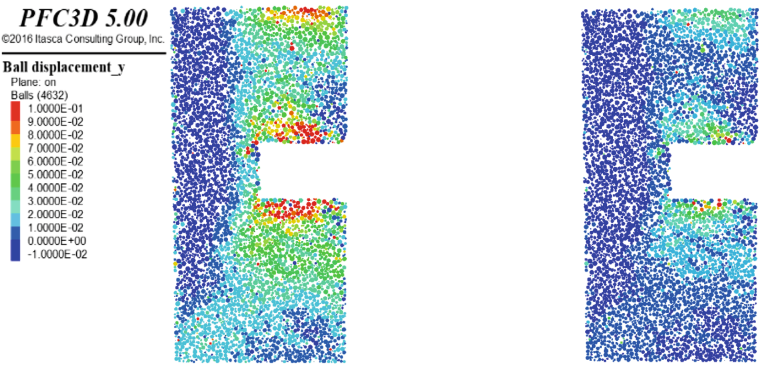

(a) λ=0.2 (b) λ=0.3

Fig. 7. Horizontal displacement of particles at different λ

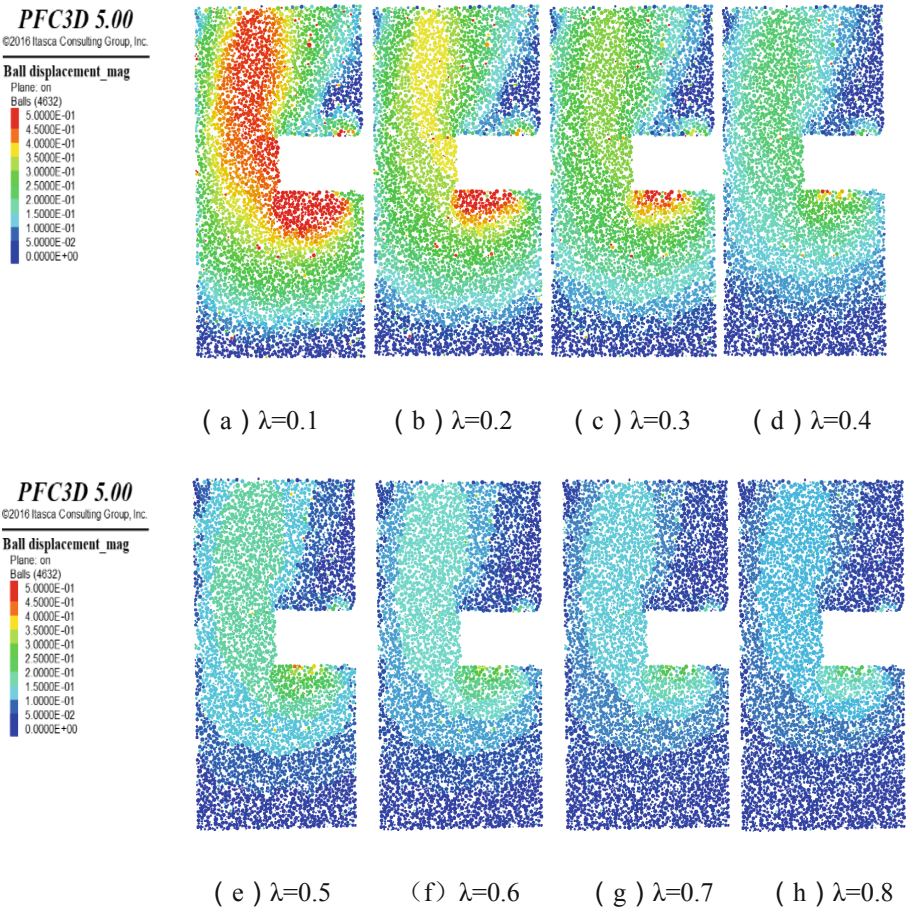

Fig. 8. Total displacement of particles at different λ

From Fig. 7, 8, we can get:

① When the stress ratio is between 0.2 and 0.3, the displacement of the particles changes greatly with the change of the stress ratio. When the stress ratio is greater than 0.3, the change of the displacement with the increase of the stress ratio is not obvious.

② There is a large displacement under the shield tunneling, because the flow field is considered and all the fluid grid outflow direction is the excavation surface. Therefore, during the excavation process, the particles below are constantly moving to the excavation surface under the action of the fluid drag force, resulting in a large displacement.

The particle displacement at the tunnel face is sorted, and the particle displacement values under different stress ratios are obtained as shown in Fig. 9. It can be seen from the figure that as the stress ratio increases, the particle displacement decreases gradually. When the stress ratio is greater than 0.3, the particle displacement value and the stress ratio basically show a linear relationship; when the stress ratio is 0.28, the curve appears

an inflection point, and then “Turn down sharply”, at this time it can be considered that the tunnel face is unstable.

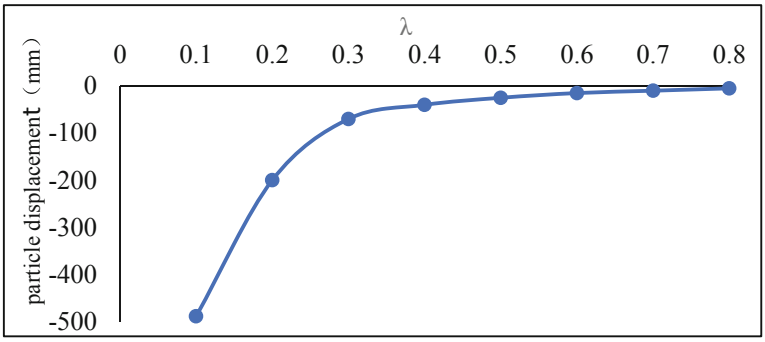

Fig. 9. Relationship between particle displacement and λ at the tunnel face

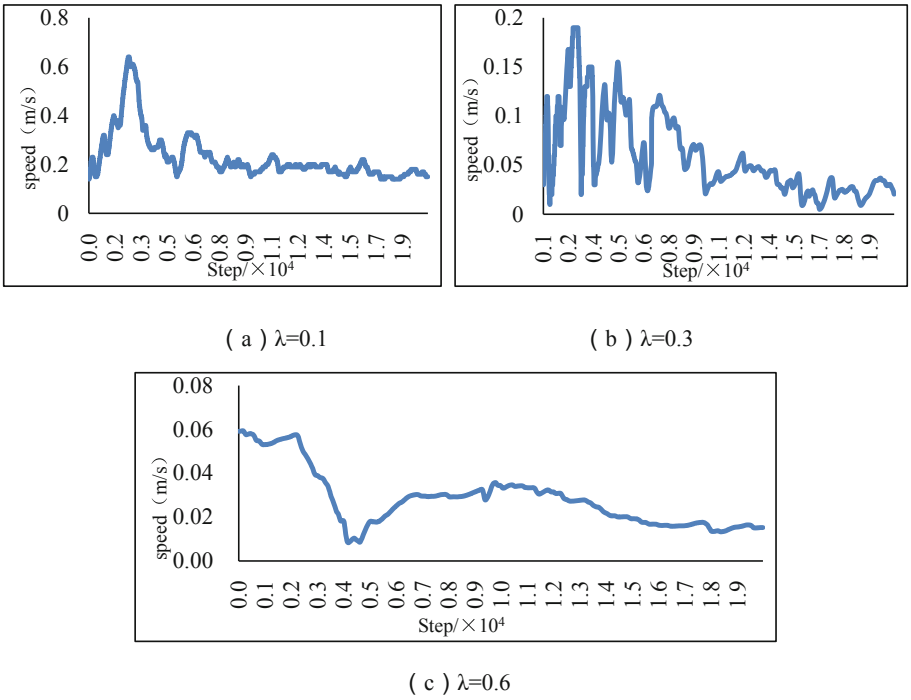

Fig. 10. Monitoring graph of particle moving speed at different λ

In addition to the particle displacement, the particle moving speed during the excavation process was also monitored. It was found that the change rule of the particle moving

speed value is basically the same as the displacement change rule. The inflection point also occurs near the stress ratio 0.28, as shown in Fig. 10. Therefore, the critical stress ratio for the working condition of 15 m buried depth and 6 m shield diameter can be set as 0.28.

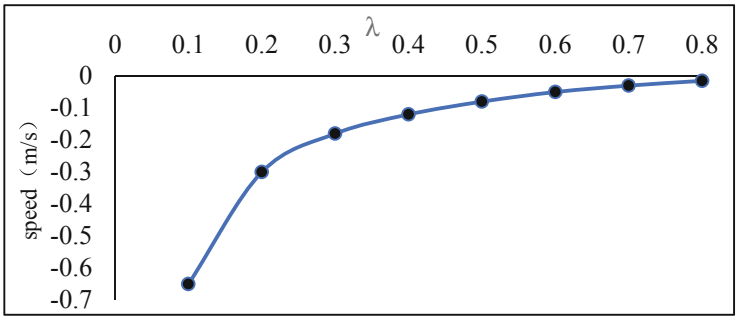

Fig. 11. Relationship between particle moving speed and λ

4.2 Influence of Shield Diameter on Stability of Tunnel Face

The section analyzes the critical stress ratio under different shield diameters (6 m, 9 m, 15 m, control buried depth is 15 m) to visually express the degree of influence. For the selection of the stress ratio in diameter 9 m and 15 m, set it with reference to diameter 6 m (working condition 1–8). The specific results are shown in Fig. 12, 13, 14, 15.

From the comparison of Fig. 12, 13, 14 and Fig. 7, 8, 9, 10, it can be seen that the larger the shield diameter, the larger the particle displacement and velocity under the same stress ratio. This shows that as the shield diameter increases, under the condition of constant burial depth, the self-stability ability of the face is weakened, and the risk of instability of the face increases.

Using the same method as Fig. 9 and 11, the critical stress ratios under the two working conditions of diameter 9 m and 15 m were obtained, and the relationship between the critical stress ratio and the shield diameter was drawn, as shown in Fig. 15.

It can be seen from Fig. 15 that the critical stress ratio also increases approximately linearly with the increase of the shield diameter, and because the buried depth is the same, the ultimate support pressure also increases linearly with the shield diameter. Therefore, when selecting shield diameter and tunneling parameters, the ultimate support pressure should be considered to avoid excessive shield diameter and mismatch of support pressure, which may cause instability of the tunnel face.

4.3 Influence on Buried Depth on Stability of Tunnel Face

This section analyzes the critical stress ratio under different buried depths (6 m, 15 m, 30 m, control shield diameter is 6 m) to visually present the effect of buried depth on the critical stress ratio and the stability of the tunnel face. The selection of related stress

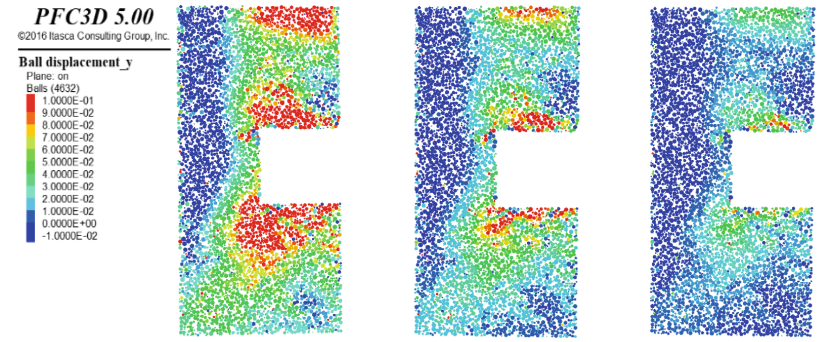

(a) λ=0.2 (D=9m)　(b) λ=0.3 (D=9m)　(c) λ=0.4 (D=9m)

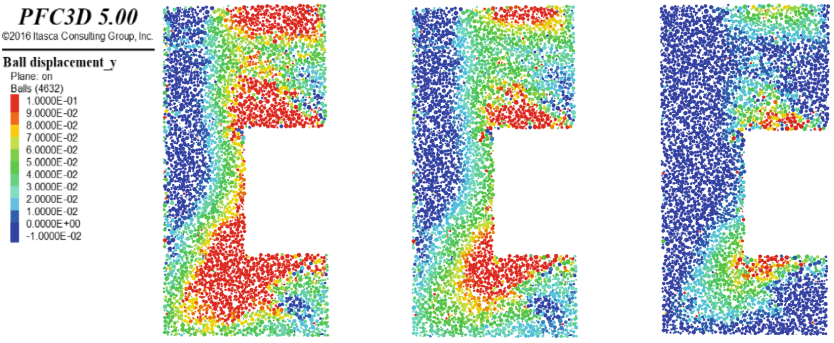

(d) λ=0.2 (D=15m)　(e) λ=0.3 (D=15m)　(f) λ=0.4 (D=15m)

Fig. 12. Horizontal displacement of particles at different D and different λ

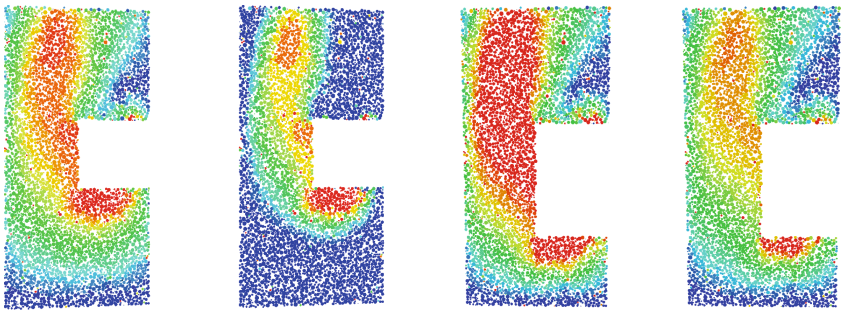

(a) λ=0.2 (D=9m)　(b) λ=0.3 (D=9m)　(c) λ=0.2 (D=15m)　(d) λ=0.3 (D=15m)

Fig. 13. Total displacement of particles at different D and different λ

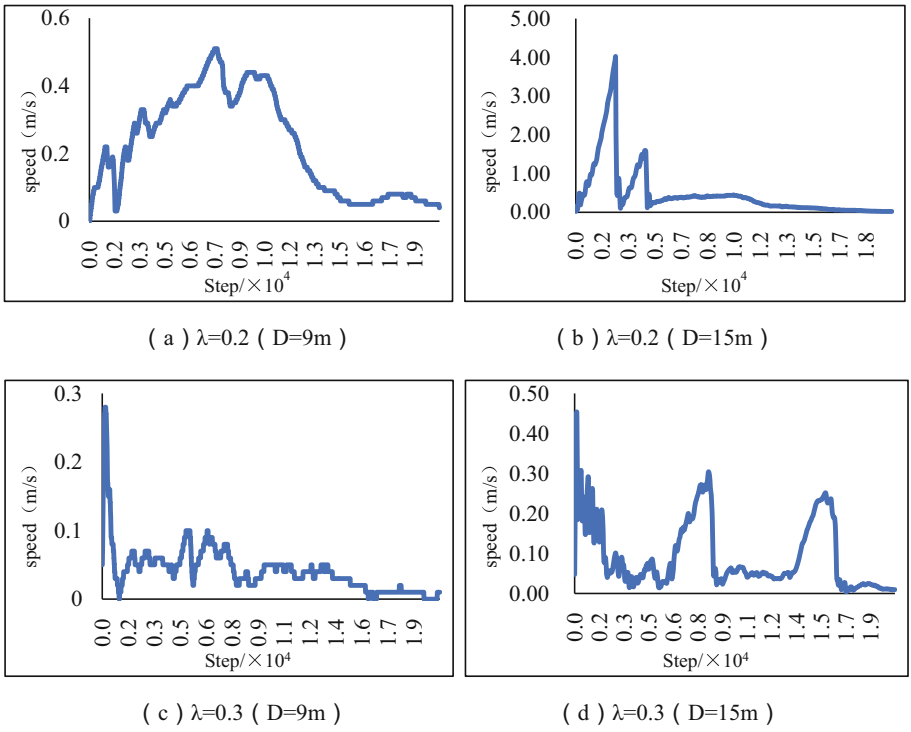

Fig. 14. Monitoring graph of particle moving speed at different D and different λ

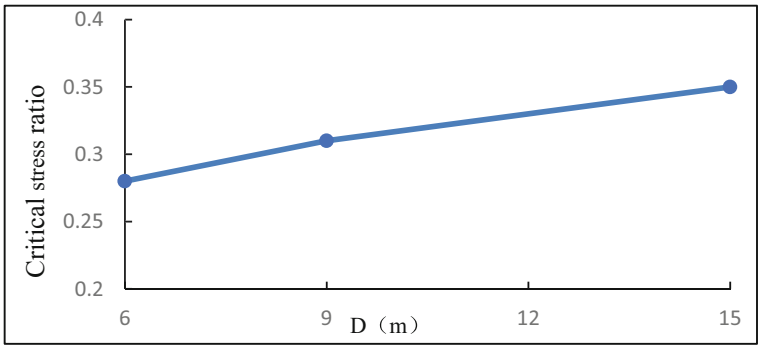

Fig. 15. Relationship between critical stress ratio and D

ratio still refers to working conditions 1–8. The specific results are shown in Fig. 16, 17, 18.

We can find that under the same stress ratio, the larger the buried depth is, the smaller the horizontal displacement of particles is, from Fig. 16 and 7. And we also find when displacement changes suddenly at the depth of 6 m, the stress radio is between 0.3 and 0.4. Moreover, when displacement change suddenly at the depth of 15 m and 30 m, the

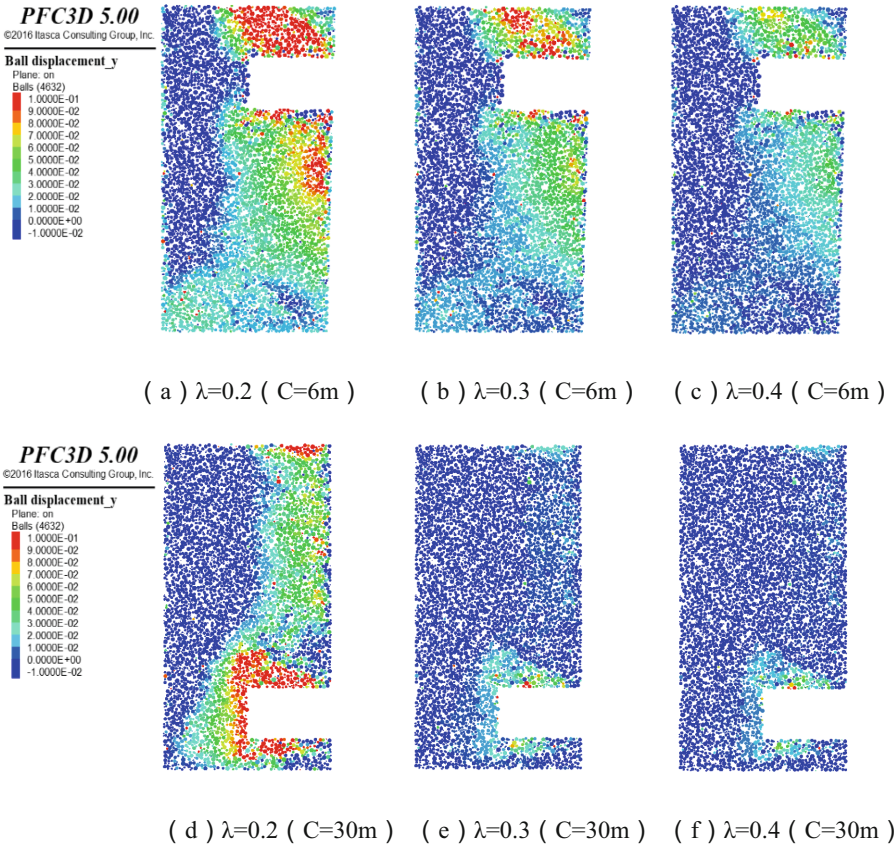

Fig. 16. Horizontal displacement of particles at different C and different λ

stress radio is between 0.2 and 0.3. And the change gonna be tiny if the stress ratio is larger than 0.3 when displacement is at the depth of 30 m. Thus, it can referred that the greater the buried depth is, the more favorable the stability of the face is. And it will not be repeated that the trend of the total displacement of particles is almost consistent with the horizontal displacement.

From the comparison of Fig. 17 and 10, it can be seen that the greater the buried depth of the shield, the smaller the particle displacement and velocity under the same stress ratio. This indicates that as the buried depth increases, the relative stability of the tunnel face increases.

This section uses the same method as Fig. 9 and 11 to obtain the critical stress ratio of different buried depths, and draws the relationship between it and the buried depth, as shown in Fig. 18.

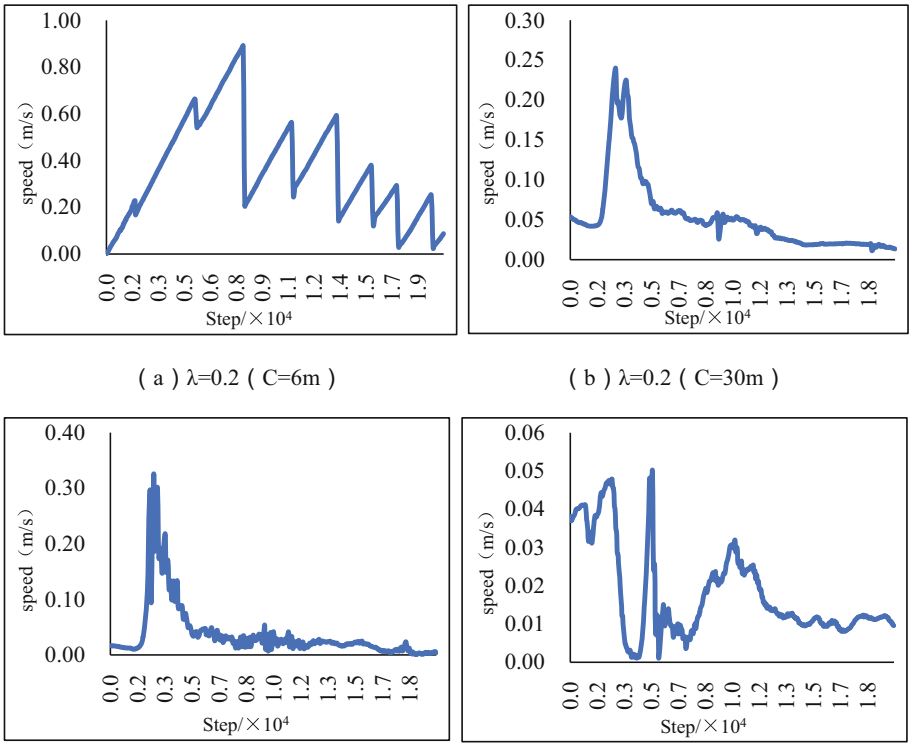

(a) λ=0.2 (C=6m)　　(b) λ=0.2 (C=30m)

(c) λ=0.3 (C=6m)　　(d) λ=0.3 (C=30m)

Fig. 17. Monitoring graph of particle moving speed at different C and different λ

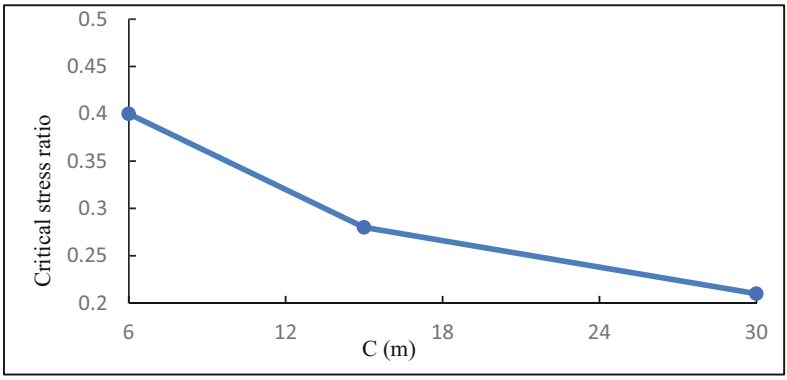

Fig. 18. Relationship between critical stress ratio and C

It can be seen from Fig. 18 that as the buried depth increases, the critical stress ratio gradually decreases, but the decreasing trend slows down and basically stabilizes at about 0.2. Although the critical stress ratio is gradually decreasing, the horizontal

stress of the formation at the tunnel face is also increasing with the depth of burial. The above two determine the size of the ultimate support pressure. The relationship between the ultimate support pressure and the buried depth is shown in Fig. 19.

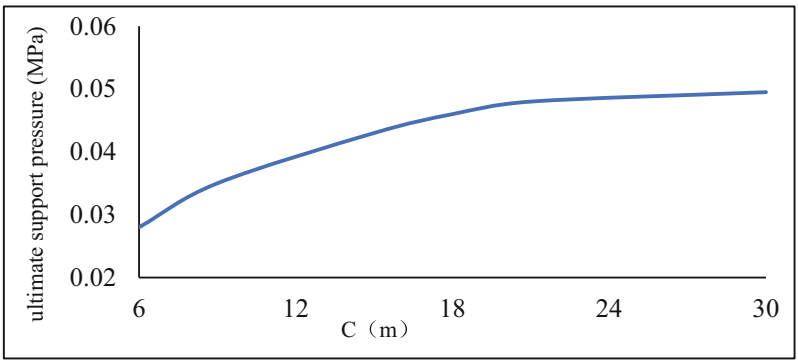

Fig. 19. Relationship between ultimate support pressure and C

It can be seen from Fig. 19 that the ultimate support pressure increases with the increase of the buried depth. When the buried depth reaches a certain value, the increase of the ultimate support pressure as the buried depth increases gradually decreases and gradually stabilizes. When C/D $>$ 3, the support pressure of the cutter-head to ensure the stability of the face is basically unchanged, and it is not necessary to blindly increase the support pressure due to the continuous increase of the buried depth.

4.4 Influence of Boulders on Stability of Tunnel Face

In actual engineering, when a boulder is encountered during shield tunneling and cannot be broken immediately, the boulder will always stay in front of the cutter head until it is broken. In this process, the cutter head is "accumulated". It will greatly increase the pressure of the cutter head, causing damage to the cutter head, and the crushing process of the boulder will form a large cavity, which may cause the instability of the face. Therefore, the following simulations are used to verify these ideas and analyze the degree of influence on the stability of the face. For this reason, working condition 13 is set, and a circular particle with a radius of 150 cm is placed on the center line of the model cutter head to simulate the influence of boulders on the stability of the tunnel face is shown in Fig. 20. Due to the high strength of general boulders, the limit of the contact force removed from boulder crushing is set at 250 kN in the model.

In the model, when encountering boulders, most of the front of the face will be occupied by boulders, but when the contact force is not enough to break it instantly, the boulders will always stay in front of the cutter head until the set contact force limit is reached. The cutter head and the boulder are in point contact. To achieve the crushing condition, the cutter head pressure will be greatly increased, as shown in Fig. 21.

It can be seen from Fig. 21 that when the excavation reaches about 9 m, the cutter head starts to contact the boulder. At this time, the cutter head pressure rises rapidly.

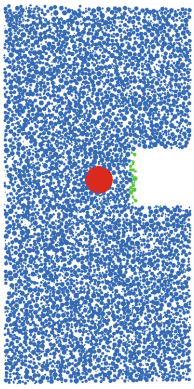

Fig. 20. Schematic diagram of boulder location

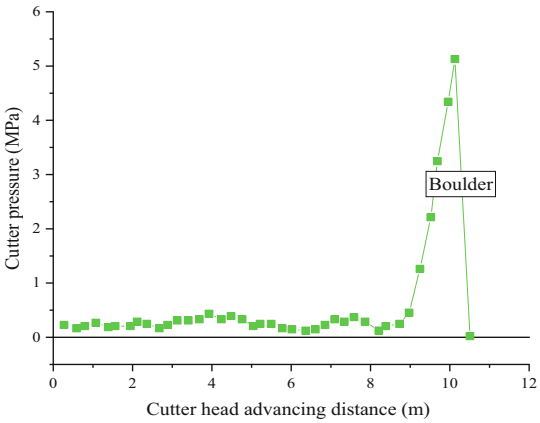

Fig. 21. Change of cutter head pressure during tunneling

After the pressure reaches the peak, it immediately decays to a value close to 0. This is because the boulder instantly It was deleted because there was no particle filling at its original location, and the contact between the cutter head and the particles decreased rapidly. This result verified the previous guess.

Comparing Fig. 22 with Fig. 8-e, it is found that the presence of boulders greatly increases the displacement of particles on the face of the tunnel, and has a greater impact on the particles of the entire formation, which greatly increases the risk of instability of the face.

It can be seen from Fig. 23 that the instantaneous horizontal velocity of the central particle of the tunnel face after the boulder is deleted is close to 3000 mm/s. Combined with Fig. 21, it can be judged that the tunnel face is at risk of instability. In general, the presence of boulders in front of the master is extremely dangerous for shield tunneling, and additional attention should be paid during construction.

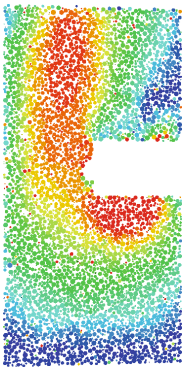

Fig. 22. Stratum displacement map after the boulder is broken

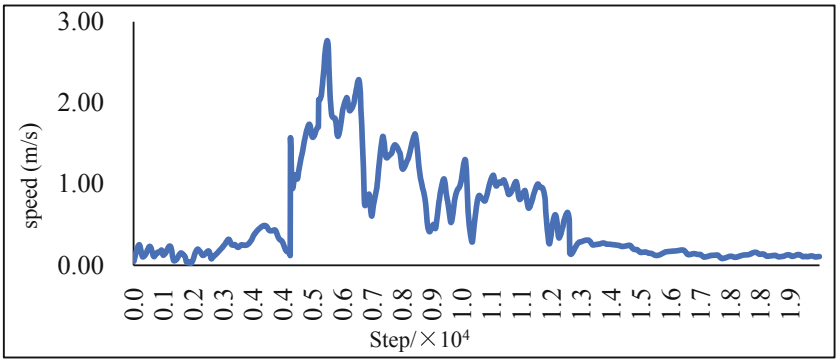

Fig. 23. Monitoring graph of particle velocity in the face

However, it needs to be pointed out that the relevant analysis in this section takes into account the engineering characteristics of sandy pebble, particle amplification effect and water seepage. Therefore, compared with the previous research results (basically between 0.15 and 0.3) obtained by most scholars in sand and other strata, the critical value obtained in this paper is higher, fluctuating around 0.3.

5 Conclusion

In this paper, combined with indoor experiments, using PFC3D to establish a numerical model, analyze the main factors affecting the stability of the shield excavation face in sand and gravel formations and their changing laws. The main conclusions obtained are as follows:

(1) The physical and mechanical properties of 5 sand pebble soil samples were tested in laboratory, and the empirical formula of permeability coefficient of sand pebble soil was obtained. PFC^{3D} mesoscopic model parameters, such as particle stiffness, density, friction coefficient and permeability coefficient, were calibrated according to laboratory test results.

(2) An indicator that can reflect the stability of the face is introduced: stress ratio (support pressure/horizontal stress of the original formation), and the influence of factors such as shield diameter, buried depth, and boulders on it is analyzed. The larger the stress ratio, the smaller the particle displacement and particle moving speed, and the more stable the formation during shield tunneling. When the stress ratio is less than the critical stress ratio, the tunnel face will lose stability.

(3) The critical stress ratio decreases with the increase of C/D, and when C/D reaches 3, the ultimate support pressure basically stabilizes.

(4) The presence of boulders greatly increases the risk of instability of the face, and the center of the face is broken immediately Particle speed can reach 3 m/s.

This paper considers the seepage problem relatively simply, such as the rough setting of the pressure gradient and the single direction of fluid inflow. On the basis of this paper, subsequent research work will consider the impact of water level changes on soil stability to study the impact of complex flow fields on shields, so as to obtain flow field parameters that are more in line with actual conditions, which will have greater guiding significance for the project.

References

1. Vermeer, P.A., Ruse, N.M., Marcher, T.: Tunnel heading stability in drained ground. Felsbau **20**(6), 8–18 (2002)
2. Zhang, C.P., Han, K.H., Zhang, D.L.: Face stability analysis of shallow circular tunnels in cohesive–frictional soils. Tunneling Underground Space Technol. **50**(8), 345–357 (2015)
3. Melis Maynar, M.J., Medina Rodriguez, L.E.: Discrete numerical model for analysis of earth pressure balance tunnel excavation. J. Geotech. Geoenviron. Eng. **131**(10), 1234–1242 (2005)
4. Chen, R.P., Tang, L.J., Ling, D.S., et al.: Face stability analysis of shallow shield tunnels in dry sandy ground using the discrete element method. Comput. Geotech. **38**(2), 187–195 (2011)
5. Karim Asm, M.: Three-dimensional discrete element modeling of tunneling. University of Alberta, Alberta (2007)
6. Wang, M.M., Wei, L.H., Lu, J.F.: Study of face stability of cobble-soil shield tunneling at Chengdu metro. Rock Soil Mech. **31**(1), 99–105 (2011)
7. Kirsch, A.: Experimental investigation of the face stability of shallow tunnels in sand. Acta Geotech. **5**(1), 43–62 (2010)
8. Chen, R.P., Li, J., Chen, Y.M.: Large-scale tests on face stability of shield tunneling in dry cohesionless soil. Chin. J. Geotechnical Eng. **33**(1), 117–122 (2011)
9. Lv, X.L., Zhou, Y.C., Li, F.D.: Centrifuge model test and numerical simulation of stability of excavation face of shield tunnel in silty sand. Rock Soil Mech. **37**(11), 3324–3328 (2016)
10. Sun, X.H., Liao, L.C., Lin, H.S.: Numerical simulation research on excavation face stability of different depths of shield tunnel. J. Southeast Univ. **47**(1), 164–169 (2017)
11. Lin, H.S.: Study on the face stability around shield tunnels and numerical simulation of PFC. Southeast University, Jiangsu (2016)
12. Li, R.J.: Stability analysis of soil pressure balance shield tunneling face in sand stratum. Beijing Jiaotong University, Beijing (2019)
13. Liu, G.L.: Research on Geological Property and Deformation Mechanism of Sandy Cobble Stratum in Chengdu Metro. Southwest Jiaotong University, Sichuan (2016)